RADIO EMISSION FROM H II REGIONS*

YERVANT TERZIAN†
Goethe Link Observatory, Indiana University; and
National Radio Astronomy Observatory,‡ Green Bank, West Virginia
Received January 4, 1965; revised February 26, 1965

ABSTRACT

Observations of IC 410, NGC 2175, M16, and NGC 6820 were made with the NRAO 300-foot radio telescope at four radio frequencies—1410, 750, 405, and 234 MHz. The derived flux densities indicate that these sources have thermal spectra. Theoretical radio spectra were computed for these sources at different electron temperatures, using the observed brightness-temperature distribution at 1410 MHz. The results show that these nebulae are still optically thin at 234 MHz. Using spherical models, one-dimensional electron-density distributions were computed at several electron temperatures. Density minima were indicated at the centers of the nebulae NGC 2175 and NGC 6820 By use of the recombination theory, Lyman continuum fluxes were derived from the radio flux densities. These were compared with the Lyman continuum fluxes derived from Hβ flux observations (for M16 and NGC 2175); the results show a very good agreement. From the theories of formation and evolution of H II regions, the ages of these nebulae were estimated to be about 50000 years, except for NGC 6820 where an age of 180000 years was estimated.

I. INTRODUCTION

The study of H II regions at radio wavelengths has mostly been performed until recently with small antennas and large beam widths. In a few cases diffuse nebulae have been resolved at centimeter wavelengths (Menon 1962). The recent theoretical developments on the formation and evolution of H II regions, and especially the construction of theoretical models (Vandervoort 1964) require an accurate empirical knowledge of these regions. In particular, reliable density distributions in diffuse nebulae are needed.

The present study deals with radio observations of four nebulae, IC 410, NGC 2175, M16, and NGC 6820, and their interpretation. These nebulae have well-defined exciting stars of different O-spectral types. In order to determine accurate spectra of these objects, observations were made at four radio frequencies—1410, 750, 405, and 234 MHz. These four nebulae have been observed by Westerhout (1958) at 1390 MHz in his survey of the galactic plane with a beam width of 35′. No detailed structure of these objects was revealed, since the sizes of these H II regions are of the order of 30′ in radius.

The exciting stars for the H II regions together with their spectral types and absolute magnitudes (from Hiltner 1956, and Rubin, Burley, Kiastapoor, Klock, Pease, Rutscheidt, and Smith 1962) are given in Table 1. The same table gives the distances for the nebulae, which have been obtained from the mean distances of the adopted exciting stars.

IC 410 contains a small cluster of early-type stars. The O-type stars that contribute most of the ionization are all within a few minutes of arc and range from O5 to O8 spectral type. The nebula NGC 2175 may be associated with the I Geminorum association. Its exciting star HD 42088 is reported by Hardie, Seyfert, and Gulledge (1960) to be a member of the I Geminorum association. In the direction of NGC 2175 there is very little absorbing matter. Its galactic latitude is about +3.4 (b^{II}). NGC 2175 has a high emission measure and has a uniform shape, except in the eastern side of this region where there is an indication of a sharp straight boundary. This feature is not due to absorption since the distribution of the radio emission shows the same characteristic. The nebula

* *Publications of the Goethe Link Observatory*, No. 63.

† Present address: Arecibo Ionospheric Observatory, Cornell University, 995 Arecibo, Puerto Rico.

‡ Operated by the Associated Universities, Inc., under contract with the National Science Foundation.

M16 is a member of the Sagittarius spiral arm of our Galaxy. A rich star cluster (NGC 6611) of early-type stars is imbedded in this H II region. Three-color photoelectric and photographic observations of stars in NGC 6611 have been made by Walker (1961). The available photometric observations show that there is in this region a large amount of reddening which is extremely variable. In general the absorption in the northern part of the region is about three times as much as in the southern part. In fact, when the radio isophotes from the present study are compared with the optical picture of the nebula (using the red prints of the *National Geographic Society–Palomar Observatory Sky Atlas*), they clearly show that the amount of reddening in the northern part of M16 should be extremely high. The optical structure of the nebula shows several conspicuous bright rims, knots, and filaments which may indicate density condensations where conditions would be most favorable for star formation.

TABLE 1

EXCITING STARS

H II Region	Distance (pc)	Exciting Star(s)	Spectral Type	M_v
IC 410	3000	BD+33°1023	O5	−5 1
		BD+33°1024	O6	−5 1
		BD+33°1026	O8	−5 1
NGC 2175	2000	HD 42088	O6	−5 1
M16	2500	HD 168076	O5	−5 5
		HD 168075	O7	−5 5
		HD 168137	O8	−5 2
		W1. 10776	O9	. . .
		BD−13°4930	O9 5	−4 4
NGC 6820	2500	BD+22°3782	O7	−5 1
		BD+22°3781	B0 IV	−4 6

NGC 6820 is associated with a very interesting young cluster of stars (NGC 6823). A chain of OB-type stars is located in the center of the cluster forming several Trapezium-type systems of very compact stellar groups. This multiple system (known as BD+22°3782) is unique in its features. According to Ambartsumian (1958) its explanation by random grouping is out of the question. This system probably presents direct evidence of the very early stages of star formation. The nebula NGC 6820 has a very small emission measure. There is strong indication of extremely variable reddening in the region of the nebula and the surroundings, which again is supported by the radio isophotes. The high-resolution radio observations of the energy distribution of this nebula has shown it to have a shape and structure completely different from its optical appearance. The radio isophotes show a striking resemblance with the radio isophotes of the Rosette Nebula (Menon 1962). This could not be seen optically because of the extremely variable and heavy reddening of this region.

II. OBSERVATIONS AND REDUCTIONS

All the observations were made at the National Radio Astronomy Observatory with the 300-foot transit radio telescope. Six feeds were installed at and near the focus of the telescope: three at 1410 MHz, one at 750 MHz, and two low frequencies at 405 and 234 MHz. Observations were made simultaneously at all frequencies. All the receivers were Dicke-type radiometers. Some parameters of the receivers and beams are given in Table

2. Direct analogue records were taken on a six-channel recorder, and the output was also recorded digitally on punched paper tape. Two of the six feeds, the 750 and one of the 1410 MHz (referred to as 1410-C) feeds were centered at the focal point, thus having a concentric feed system. The remaining two 1410 MHz (referred to as 1410-E and 1410-W) feeds were mounted NW. and SE. from the center. The low-frequency feeds (helices with ground planes) were installed as close as possible to the focal point, one NE. and the other SW. of the center.

During the course of the observations, the shapes of all the beams were determined by making observations of a strong point source at slightly different declinations. The central beams were found to be fairly symmetrical, but each of the 1410-E and 1410-W beams had one small sidelobe. The low-frequency beams were slightly asymmetrical due to the fact that the feeds were off-center, but no sizable sidelobes were present in these cases. The half-power beam widths (HPBW) of the main beams in declination and right ascension were measured from the contour maps of the beams and are given in Table 2. Daily observations of two or more standard sources were made with each system. A thermal calibration was taken before and after each observation. The standard sources

TABLE 2

PARAMETERS OF THE RECEIVERS AND BEAMS

ν (MHz)	$HPBW_\delta$ (Min of Arc)	$HPBW_\alpha$ (Min of Arc)	Band Width (MHz)	Radiometer Temperature (° K)	Standard Source	S_ν (10^{-26} W m^{-2} Hz^{-1})
1410-C	10 0	10 0	8	190	3C 71	5 460
1410-E	10 8	10 0	8	138	3C 196	14 886
1410-W	10 2	12 0	8	210	3C 196	14 886
750	18 8	18 8	6	450	3C 71	7 410
405	45 0	43 0	4	875	3C 353	130 0
234	67 0	65 0	4	1000	3C 353	184 0

were normalized to the thermal calibration, and a least-squares linear fit was put through the points. 3C 71 was adopted as a standard for the 1410-C and 750 MHz systems; 3C 196 was used for the 1410-E and 1410-W systems; and 3C 353 was used for the low-frequency systems. The flux densities of these sources were obtained from Conway, Kellermann, and Long (1963).

The flux density of a standard point source can be written as

$$S_{\lambda,\mathrm{st}} = \frac{2k}{\lambda^2}\frac{T_{\mathrm{cal}}}{E_b}\int_{\mathrm{main\ beam}}\frac{D_{\mathrm{st}}}{D_{\mathrm{cal}}}\,d\Omega\,, \tag{1}$$

where k is the Boltzmann constant, λ is the wavelength, E_b is the beam efficiency, and $D_{\mathrm{st}}/D_{\mathrm{cal}}$ is the normalized deflection of the standard source. The main beam solid angle can be represented by a Gaussian function and can be written as $1.133\,\theta_\alpha\theta_\delta$, where θ_α and θ_δ are the HPBW in right ascension and declination. Therefore we can write

$$\frac{T_{\mathrm{cal}}}{E_b} = \frac{S_{\lambda,\mathrm{st}}}{2k}\left(\frac{D_{\mathrm{st}}}{D_{\mathrm{cal}}}\right)^{-1}\frac{1}{1.133\,\theta_\alpha\theta_\delta}\,. \tag{2}$$

The ratio T_{cal}/E_b when multiplied by the normalized deflection of any observed point gives the brightness temperature T_b of that point. In the case of the two off-center 1410 MHz beams, a correction was made to the half-power beam widths of the main beams in order to include the contribution of the sidelobes in deriving the flux density of extended sources. By integrating the sidelobes and main beams separately, the contribution of the sidelobes for the 1410-E system was found to be 4.6 per cent, and that of the 1410-W system 3.6 per cent.

The observations were spaced by 5′ in declination at 1410 MHz, 10′ or closer at 750 MHz, and about 10′–20′ at the low frequencies. The right-ascension range varied from source to source. In the cases of NGC 6820 and M16, a single transit covered more than 1 hour in right ascension. Most of the observations were repeated at least three times for increased accuracy. The integration time of every observed point was 10 seconds. A comparison of observations at the same declination and right-ascension range with the three 1410 MHz systems showed no significant lack of resolution for the off-center systems. All the observations were reduced from the punched tape records using an IBM 1620 II computer. The observations were normalized to the calibration signals and were

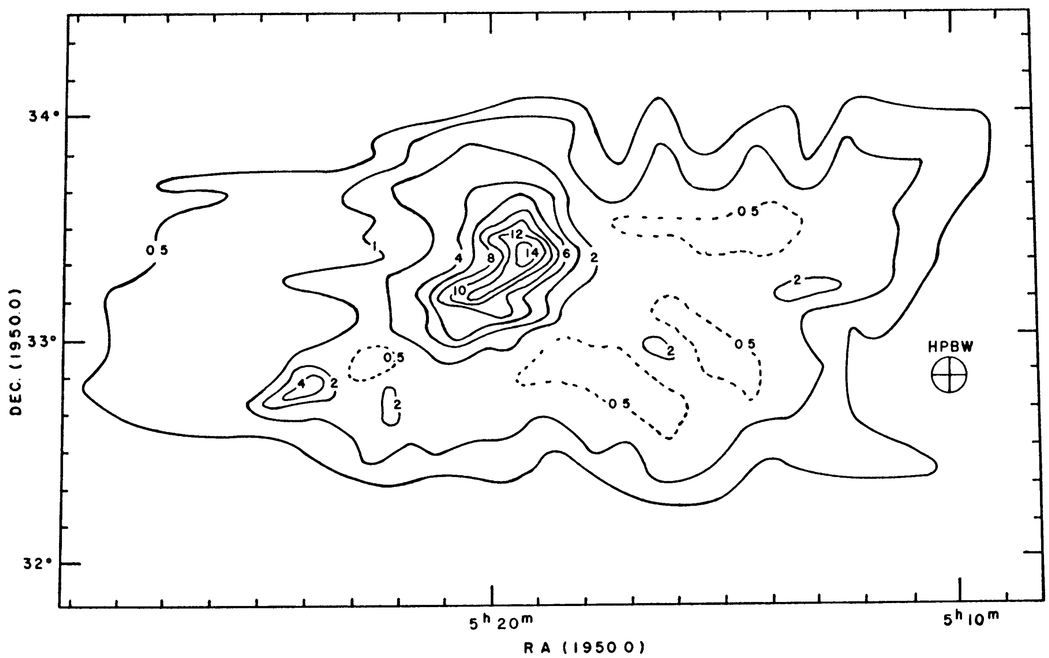

FIG. 1.—Equal brightness-temperature contours at 1410 MHz for the region of IC 410

plotted on a magnified scale with a line printer. The plots were examined to decide about any receiver drift during the course of an observation. The drift was considered to be linear and was taken out by fitting a straight line between the averages of two ranges of points near the beginning and end of an observation. This baseline was considered to be the zero-temperature line. Multiplication of each observed point with the respective value of T_{cal}/E_b gave the brightness-temperature of that point. The observations were then averaged, and the final brightness-temperature distributions of the observed regions were obtained. The observations were also corrected for beam width using Bracewell's (1955) method. From the above results contours of equal brightness temperatures were drawn for each observed region at 1410 MHz. These are shown in Figures 1–4. The flux densities of the nebulae were then computed using Bracewell's (1956) method. For the determination of the flux densities of M16 and NGC 6820 the background contribution of the galactic plane was subtracted from the final brightness-temperature distributions. This was performed independently for each averaged brightness-temperature drift-curve by assuming the size of the H II region at every observed declination from the drawn contour maps. The background for IC 410 and NGC 2175 was considerably smaller. Table 3 gives the derived flux densities at the four frequencies for all four sources.

The uncertainties of the measured flux densities arise from several causes. The statistical random errors of the brightness temperature contribute a small part of the total error. Part of the uncertainty is introduced by the process of the calibration and the uncertainty of the adopted flux densities of the standard sources. This error is at most ± 4 per cent at the high frequencies and about ± 6 per cent at the low frequencies. The errors produced by subtracting the background brightness temperature have been estimated separately for each source and for each frequency.

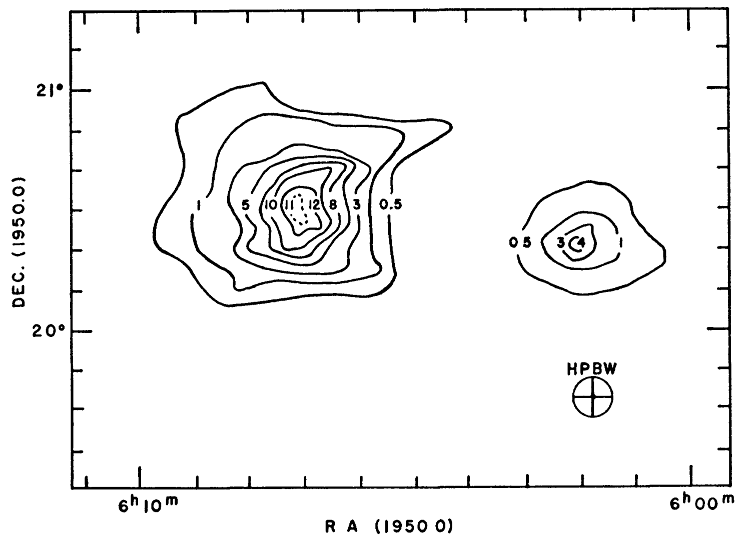

FIG. 2.—Equal brightness-temperature contours at 1410 MHz for the region of NGC 2175. The smaller source is 3C 152.

TABLE 3

FLUX DENSITIES

ν (MHz)	S_ν (in units of 10^{-26} W m^{-2} Hz^{-1})			
	IC 410	NGC 2175	M16	NGC 6820
1410	68 ± 4	43 ± 3	170 ± 7	50 ± 5
750	62 ± 7	39 ± 5	181 ± 8	53 ± 6
405	64 ± 9	51 ± 5	194 ± 15	50 ± 9
234	56 ± 10	44 ± 7	160 ± 20	61 ± 7

III. PHYSICAL PROPERTIES OF THE NEBULAE

a) *Theoretical Spectra*

It is well understood that the radio radiation emitted by diffuse nebulae is of thermal character and is due to the free-free transitions from a hydrogen plasma. The most recent results for the absorption coefficient from an ionized plasma are given by Oster (1961). It can be shown that the absorption coefficient K_ν is

$$K_\nu = 9.776\times10^{-15}\frac{N_e^2}{\nu^2 T_e^{3/2}}\ln\left[49.503\frac{T_e^{3/2}}{\nu}\right], \tag{3}$$

1965ApJ...142..135T

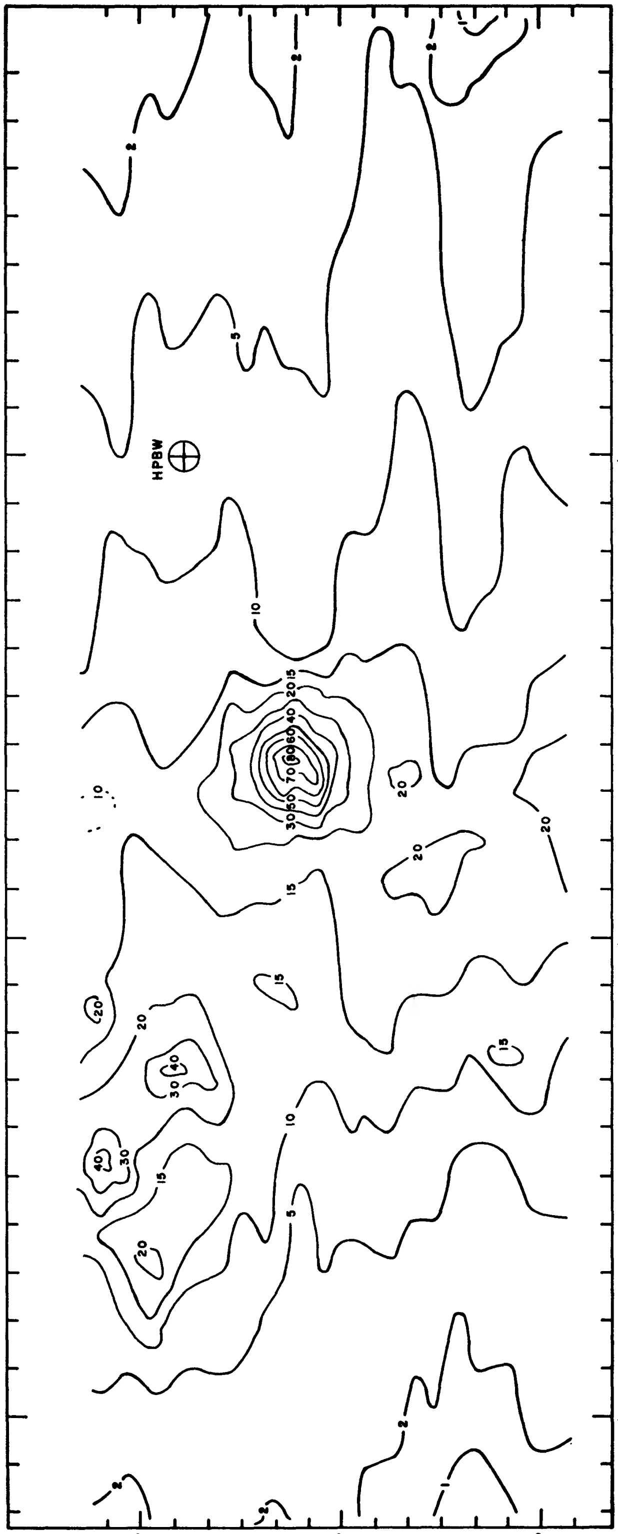

FIG. 3.—Equal brightness-temperature contours at 1410 MHz for the region of M16

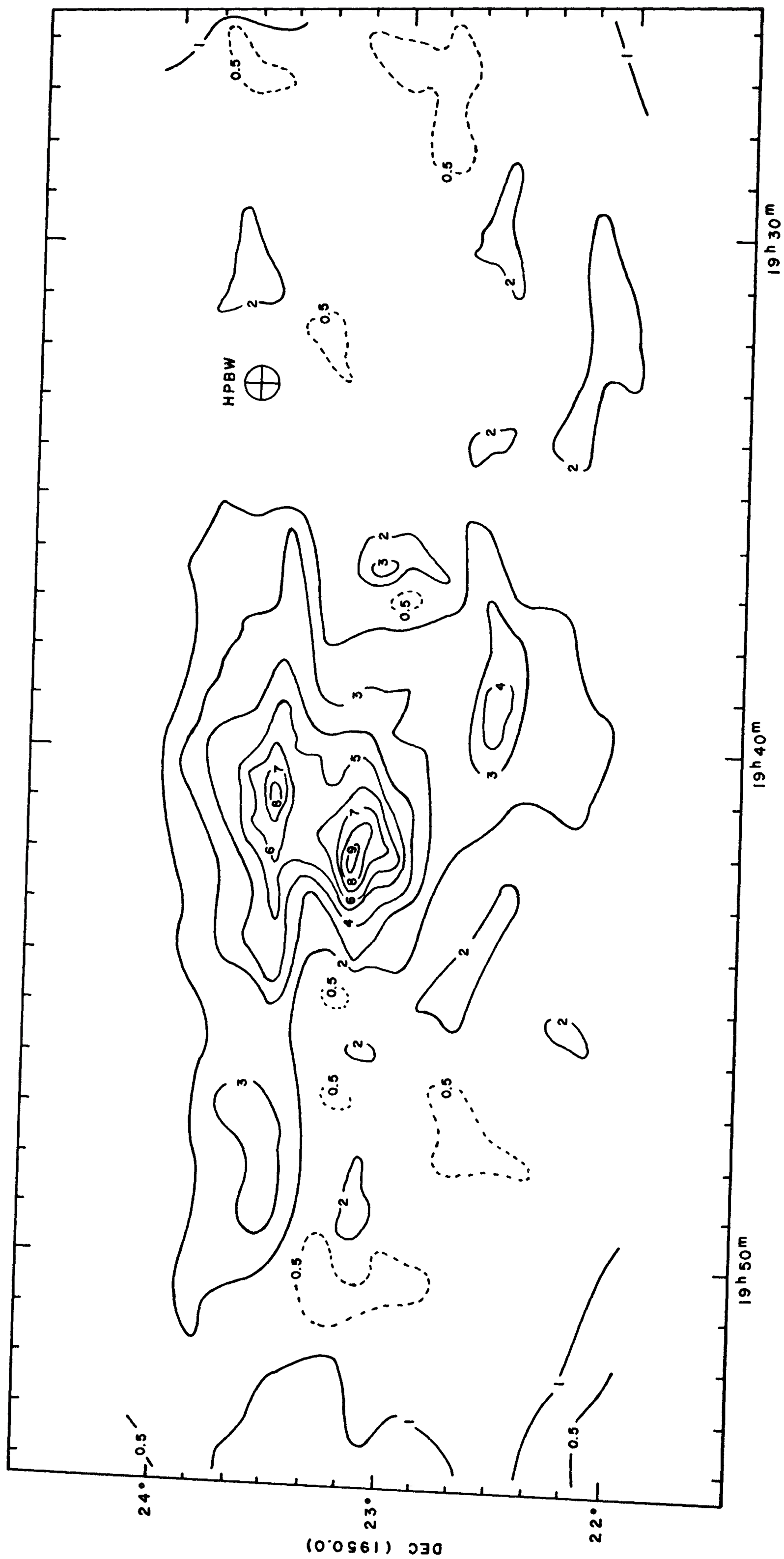

FIG. 4.—Equal brightness-temperature contours at 1410 MHz for the region of NGC 6820

where N_e is the electron density, T_e is the electron temperature, and ν is the frequency in MHz.

If the brightness-temperature distribution over an ionized hydrogen cloud is known from observations at a high frequency, where the approximation $\tau_\nu(r) = T_b(r)/T_e$ can be used for the optical depth, then by assuming an electron temperature we can compute the optical depth distribution over the source at that frequency. We can then easily compute the optical depth distribution at a second frequency. With this new optical depth distribution we can use

$$T_b(r) = T_e(1 - e^{-\tau_\nu(r)}) \tag{4}$$

to compute a new brightness-temperature distribution at the second frequency and hence a theoretical flux density. Thus we can derive the theoretical radio spectrum of a

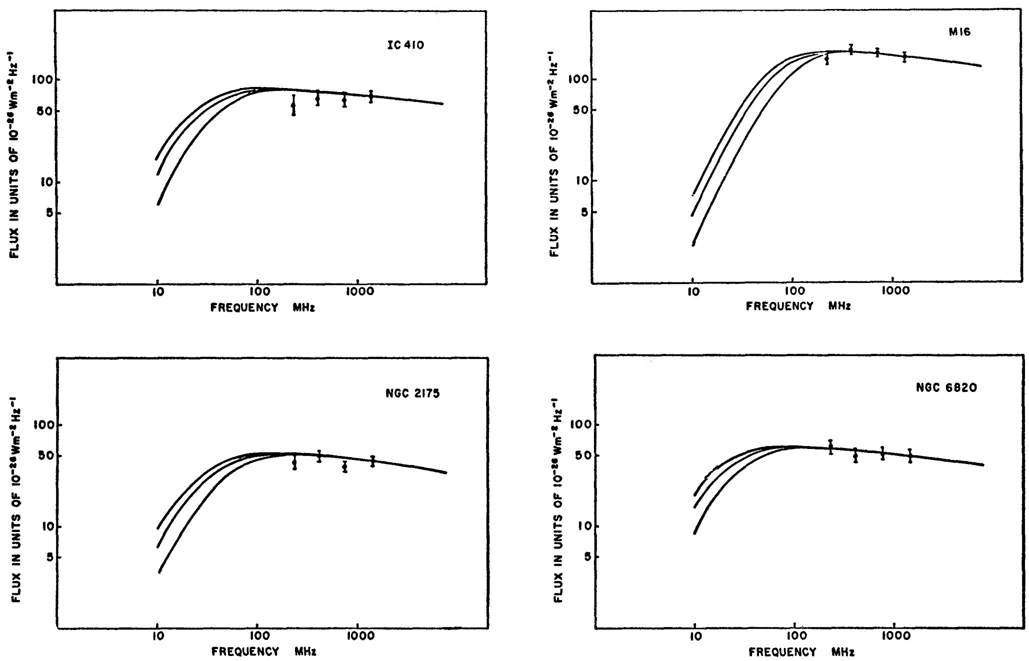

Fig. 5.—Computed and observed radio spectra for IC 410, NGC 2175, M16, and NGC 6820. The three solid curves show the computed radio spectra for $T_e = 5000°$ (innermost curve), 10000° and 15000° K.

diffuse nebula. The electron temperature can be varied and the above procedure can be repeated. The best mean electron temperature will obviously be the one which gives the best match of the theoretical radio spectrum with the observed one.

The final brightness-temperature distributions at 1410 MHz of the four H II regions were adopted for the theoretical calculations of the radio spectra of these sources. At this frequency all these objects are optically thin. Theoretical spectra for each nebula were calculated for electron temperatures ranging from 5000° to 15000° K with 1000° intervals. Flux densities were calculated at twelve frequencies from 8000 to 10 MHz. In Figure 5 the observed flux densities are compared with the theoretical results. From these comparisons we can deduce that the emission of all four nebulae is due to thermal radiation. It is clear from the four spectra that these regions are still optically thin even at 234 MHz. Hence no electron temperature determinations can be made at present. Accurate observations below 50 MHz are necessary in order to discriminate between different electron temperature values.

b) Density Distributions and Masses

The density distributions of the H II regions were derived by assuming spherical models for the ionized regions. The radio isophotes seem to indicate that this is a reasonable approximation. In the case of NGC 6820 the center of the model was chosen to be between the two energy peaks, which corresponds to the center of the star cluster. The stars capable of ionizing this region are all located very close to the adopted center of the nebula.

The radio maps of the H II regions were divided into concentric shells with intervals of 2′. The sizes of the regions were estimated from the radio isophotes and are given in Table 4. The models were divided into sixteen radii and the mean brightness temperature for each shell was found. By use of the derived one-dimensional brightness-temperature distribution and spherical models, theoretical spectra were calculated as described in the previous section. These spectra were compared with the ones derived using the two-dimensional brightness-temperature distributions. An agreement of better than 1 per cent was found.

TABLE 4

RADII AND MASSES

H II REGION	RADIUS		$M/M_{\odot}$
	Min of Arc	pc	
IC 410	28	24 4	14,000
NGC 2175 . .	30	17 4	4,000
M16. . .	28	20 3	12,500
NGC 6820 .. .	38	27.6	12,000

From the definition of the optical depth and the expression for the absorption coefficient we have

$$\tau_\nu = \frac{\zeta}{\nu^2 T_e^{3/2}} \int_0^s N_e^2 ds\,, \tag{5}$$

where ζ is a slowly varying function of ν and T_e. Using the approximation $\tau_\nu(r) = T_b(r)/T_e$, we can write

$$\int_0^s N_e^2 ds = \frac{\nu^2 T_e^{1/2} T_b(r)}{\zeta}. \tag{6}$$

From the last expression, one-dimensional density distributions were computed for the four H II regions assuming a constant density within each shell, and using the one-dimensional brightness-temperature distributions. These computations were performed for three electron temperatures, 5000°, 10000°, and 15000° K. The results are shown in Figure 6. NGC 2175 and NGC 6820 show a decrease in density toward their centers. In general no striking similarity between the density distributions of the four H II regions is found. Clearly, the densities of these regions are not uniform. Masses of the four nebulae were derived using the results of the density distributions and considering these clouds as being composed only of pure ionized hydrogen. Table 4 gives the derived masses in solar units.

c) Comparison between Optical and Radio Data

From the emission coefficient of Hβ and the emission coefficient at a radio frequency due to free-free transitions we can show that the emission ratio at a radio frequency to Hβ is

$$\frac{j_\nu}{j_\beta} = \frac{N_i}{N_p} \frac{T_e}{\langle b_4 \rangle} \frac{1.664 \times 10^{-19}}{e^{0\ 986 \times 10^4 / T_e}} \ln\left(49.503 \frac{T_e^{3/2}}{\nu}\right). \tag{7}$$

The effective value of $\langle b_4 \rangle$ for the $4 \rightarrow 2$ transition is given by Burgess (1958). We shall adopt a value of 0.200 for $\langle b_4 \rangle$. The ratio of the emission coefficients also depends on the density of ions and protons. Generalizing the results by Mathis (1951) for the Orion Nebula, we have $N_i/N_p = 1.13$. This takes into account the presence of helium atoms to a fair approximation. Since the diffuse nebulae are optically thin at Hβ and at the centimeter wavelengths in the radio continuum (Osterbrock and Stockhausen 1961), the ratio j_ν/j_β is also the ratio of the emergent fluxes at the corresponding wavelengths. Osterbrock and Stockhausen (1960) have reported an Hβ flux for NGC 2175 of 6.8×10^{-9} erg/cm^2 sec. And Boyce (1963) has reported an Hβ flux for M16 as 45.4×10^{-9} erg/cm^2

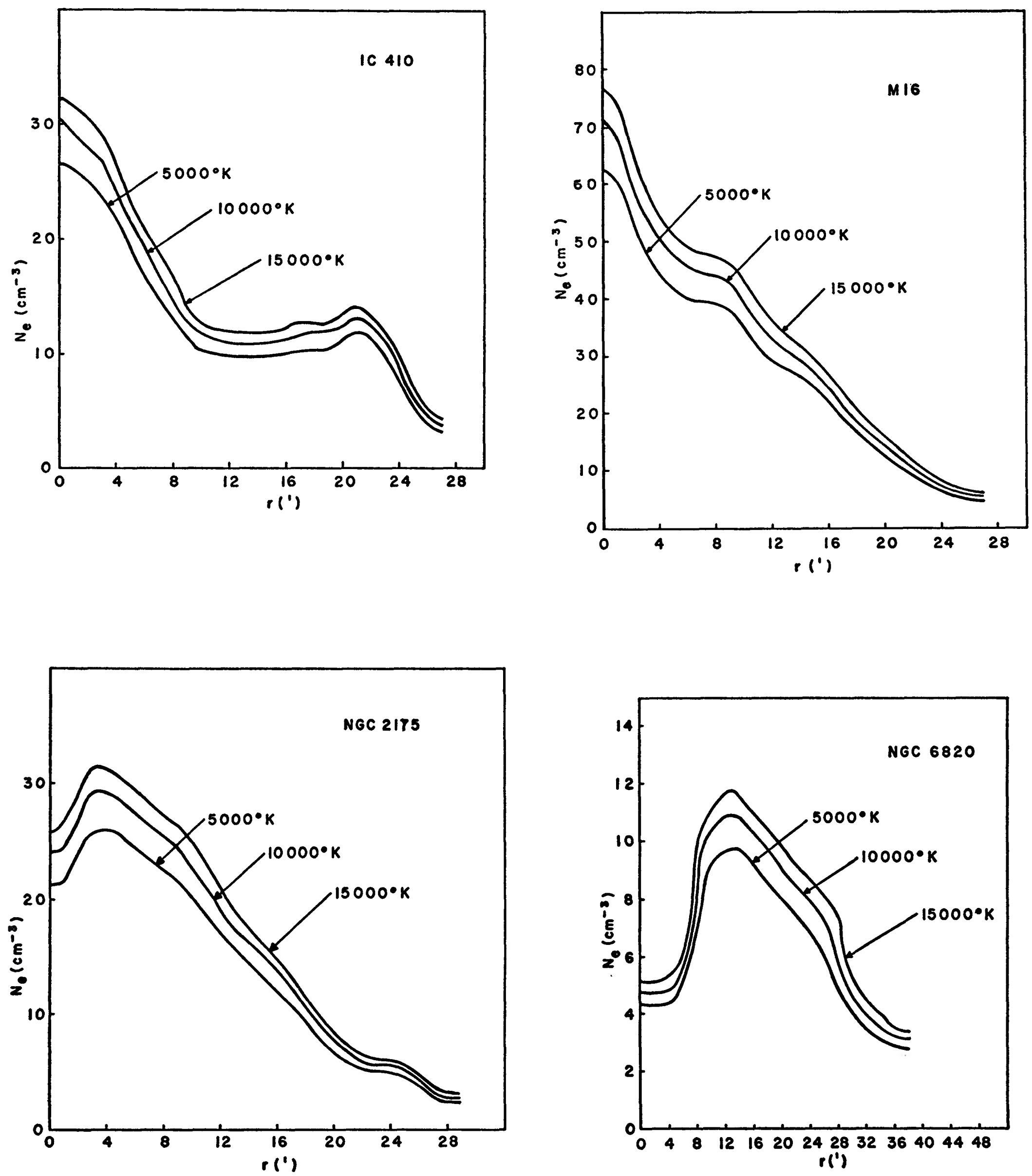

FIG. 6.—Electron density distributions at three electron temperatures for IC 410, NGC 2175, M16, and NGC 6820.

sec. Computing the ratio j_ν/j_β for a temperature of 10000° K and a radio frequency of 1410 MHz we have

$$\frac{j_\nu}{j_\beta} = 3.7 \times 10^{-14} . \quad (8)$$

Using the Hβ fluxes together with the fluxes at the 1410 MHz determined from the present study, we get 6.3×10^{-14} in the case of NGC 2175, and 3.8×10^{-14} in the case of M16. Part of the disagreement in the case of NGC 2175 may be due to the correction of interstellar absorption on the measured Hβ flux.

Following Osterbrock and Stockhausen (1960) we can compute the ratio of the Lyman-continuum photons emitted per unit volume to the number of Hβ photons, $Q_{\rm LC}/Q_\beta$. This ratio is 9.2 for a temperature of 10000° K. It is also possible to compute the ratio $Q_{\rm LC}/Q_\nu$ of ionizing photons absorbed by hydrogen to continuum photons emitted per cycle per second at a radio frequency. We can compute $Q_{\rm LC}$ from the radio flux densities at 1410 MHz for each of the four nebulae and then we can compare these results with the $Q_{\rm LC}$ values derived from the Hβ flux measurements in the cases of NGC 2175 and M16. The measured flux densities S_ν in the units of ergs/cm² Hz⁻¹ should be divided by $h\nu$ to

TABLE 5

LYMAN CONTINUUM QUANTA

H II Region	Q_{1410} (Photons/cm² sec Hz⁻¹)	$Q_{\rm LC}$ Radio (Photons/cm² sec)	$Q_{\rm LC}$ Hβ (Photons/cm² sec)	Q_v (Photons/cm² sec 1000 Å)	$Q_{\rm LC}/Q_v$
IC 410 ..	0 73×10^{-4}	4 1×10^{4}	. . ..	3 26×10^{3}	12 6
NGC 2175	0 46×10^{-4}	2 6×10^{4}	1 5×10^{4}	2 96×10^{3}	8 8
M16 .	1 82×10^{-4}	10 3×10^{4}	10 2×10^{4}	9 57×10^{3}	10 8
NGC 6820	0 54×10^{-4}	3 1×10^{4}	.	3 21×10^{3}	9 7

give Q_ν, the number of photons/cm² sec Hz⁻¹. Making use of the calculated ratio j_ν/j_β we have for Q_ν/Q_β

$$\frac{Q_\nu}{Q_\beta} = \frac{j_\nu/h\nu}{j_\beta/h\nu_\beta} = 16.2 \times 10^{-9} \quad (9)$$

at 1410 MHz. From theoretical considerations $Q_{\rm LC}/Q_\beta = 9.2$ and therefore $Q_{\rm LC}/Q_\nu$ is 0.57×10^9. The values of Q_{1410} and $Q_{\rm LC}$ for the four nebulae are given in Table 5.

The visual photon fluxes of all the exciting stars in a nebula can be added, giving Q_v. Then the ratio $Q_{\rm LC}/Q_v$ can be calculated and can be compared with the ratio derived from model atmospheres of early-type stars. Table 5 gives the quantity Q_v and the ratio of $Q_{\rm LC}$ (radio)/Q_v. The comparison with the models of early-type stars (Underhill 1950, 1951; Traving 1957) show a satisfactory agreement.

The radio sizes of the four H II regions were compared with the ones predicted by Strömgren's (1939) theory corrected for scattering according to Pottasch (1960). The results indicate good agreement except in the case of IC 410, a nebula which may be density-bounded.

IV. DISCUSSION

The results that have been obtained for the density distributions of the four H II regions indicate that the densities in these regions are not uniform. As shown in an earlier section, a density minimum has been deduced at the centers of the diffuse nebulae NGC 2175 and NGC 6820. These central density depressions may be interpreted as the result of a shock moving outward behind the ionization front (Goldsworthy 1961). From the resolution of the observations we can put an upper limit of 4′ for the radii of the shocks of M16 and IC 410. Following Kahn and Menon (1961), who have used Goldsworthy's theory, we can compute the time since the beginning of the ionization. Table 6 gives the derived estimates of the ages of the four nebulae. The derived ages are very plausible, in fact, the ages of the Rosette and Orion nebulae are about 50000 and 10000 years, respectively, which are of the same order as three of the nebulae reported here.

If we assume a mean expansion velocity $\langle v_s \rangle$ of 10 km/sec for the shock front in a nebula, we can then estimate the time since the beginning of expansion of the shock front. This time is given in Table 6 and can be compared with the time derived from the previous method. There is a disagreement by a factor of about 5, but we still have a confirmation of the young ages of the objects. It is interesting to note that, for the nebulae which are excited by O5 spectral-type stars (M16 and IC 410), no density depressions were resolved. The spectral type of the exciting star of NGC 2175 is O6, and the radius of the shock is 2.32 pc. Considering NGC 6820 with an O7 spectral-type exciting star we have 9.43 pc for the radius of the shock. It seems that there may be a correlation between the radius of the shock in a nebula and the spectral type of the exciting star, and hence with the stellar age of the exciting star.

TABLE 6

AGES OF H II REGIONS

H II Region	Age (years) (Kahn and Menon Method)	Age (years) ($\langle v_s \rangle = 10$ km/sec)
IC 410	$< 63\times10^3$	$<340\times10^3$
NGC 2175	44×10^3	230×10^3
M16	$< 53\times10^3$	$<280\times10^3$
NGC 6820	180×10^3	920×10^3

We can conclude that the shapes and sizes of ionized regions can best be determined from radio observations since they are not affected by interstellar absorption. The study of the density distributions of ionized hydrogen can lead to important discoveries about the formation of early-type stars. From the present study we can also conclude that the galactic plane around M16 and NGC 6820 is not uniform. The spiral arms of the Galaxy do not seem to have a uniform and continuous structure; rather they seem to break down into smaller sections.

The author wishes to thank Dr. T. K. Menon for his constant advice throughout this project and for reading the manuscript.

REFERENCES

Ambartsumian, V. A. 1958, *Rev. Mod. Phys.*, **30**, 944.
Boyce, P. 1963, thesis, University of Michigan.
Bracewell, R. N. 1955, *Australian J. Phys.*, **8**, 54.
———. 1956, *ibid.*, **9**, 297.
Burgess, A. 1958, *M.N.*, **118**, 477.
Conway, R. G., Kellermann, K. I., and Long, R. F. 1963, *M.N.*, **125**, 261.
Goldsworthy, F. A. 1961, *Phil. Trans. R. Soc. London*, **A253**, 277.
Hardie, R. H., Seyfert, C. K., and Gulledge, I. S. 1960, *Ap. J.*, **132**, 361.
Hiltner, W. A. 1956, *Ap. J. Suppl.*, **2**, 389.
Kahn, F. D., and Menon, T. K. 1961, *Proc. Nat. Acad. Sci.*, **47**, 1712.
Mathis, J. S. 1957, *Ap. J.*, **125**, 328.
Menon, T. K. 1962, *Ap. J.*, **135**, 394.

Oster, L. 1961, *Ap. J* , **134**, 1010.
Osterbrock, D. E., and Stockhausen, R. E. 1960, *Ap. J* , **131**, 310.
———. 1961, *ibid.*, **133**, 2.
Pottasch, S. R., 1960, *Ap. J.*, **132**, 269.
Rubin, C. V., Burley, J., Kiastapoor, A., Klock, B , Pease, G , Rutscheidt, E., and Smith, C. 1962, *A J.*, **67**, 491.
Strömgren, B 1939, *Ap. J.*, **89**, 526.
Traving, G. 1957, *Zs. f. Ap.*, **41**, 215.
Underhill, A. B. 1950, *Pub. Copenhagen Obs* , No. 151.
———. 1951, *Pub. Dom. Ap. Obs.*, **8**, 357.
Vandervoort, O. P. 1964, *Ap. J.*, **139**, 869.
Walker, M. F. 1961, *Ap. J.*, **133**, 438.
Westerhout, G. 1958, *B.A.N.*, **14**, 215.